SUPPLEMENTAL MATERIAL

Exercise-induced changes in glucose metabolism promote physiologic cardiac growth

Andrew A. Gibb[1, 2, 3], Paul N. Epstein[4], Shizuka Uchida[5], Yuting Zheng[1,2], Lindsey A. McNally[1,2], Detlef Obal[2,6], Kartik Katragadda[1,2], Patrick Trainor[1,2], Daniel J. Conklin[1,2], Kenneth R. Brittian[1,2], Michael T. Tseng[7], Jianxun Wang[8], Steven P. Jones[1,2], Aruni Bhatnagar[1,2], and Bradford G. Hill[1,2,3]

[1]Institute of Molecular Cardiology, [2]Diabetes and Obesity Center, [3]Department of Physiology, [6]Department of Anaesthesiology, [7]Department of Anatomy and Neuroscience, and [4]Department of Pediatrics, [5]Cardiovascular Innovation Institute, University of Louisville, Louisville, KY, [8]Department of Medicine, Beth Israel Deaconess Medical Center, Harvard Medical School, Harvard Medical School, Boston, MA

Table of Contents

A. Detailed Methods

Experimental Animals: All procedures were approved by the University of Louisville Institutional Animal Care and Use Committee. The mice used in this study include transgenic mice expressing a kinase-deficient (kd) form of PFK2 under the control of the α-MHC promoter (i.e., Glyco^{Lo} mice), transgenic mice expressing a phosphatase-deficient form of PFK2 under the control of the α-MHC promoter (i.e., Glyco^{Hi} mice), and wild-type (WT) littermates.[1, 2] Male mice on the FVB/NJ background were used for all studies, except for F-2,6-P_2 measurements in isolated cardiomyocytes, where both male and female mice were used. All studies began at 15 weeks of age; food and water were provided *ad libitum*; and the mice were maintained on a 12:12-h light-dark schedule, as described previously.[3] At the conclusion of animal experiments, and following a 6 h fast, mice were anaesthetized with sodium pentobarbital (150 mg/kg, i.p.), followed by euthanasia via excision of the heart. These procedures are consistent with the AVMA *Guidelines on Euthanasia*.

Exercise Capacity Testing: Mice were familiarized to the motorized rodent treadmill (Columbus Instruments, Columbus OH) on the Wednesday and Thursday before the first week of training. Familiarization consisted of an initial 10 min period where the treadmill speed and incline were

set to zero with shock grid settings of 25 V, 0.34 mA, and 2 Hz. The treadmill speed was then increased steadily to 10 m/min (Wed) and 12 m/min (Thurs) for an additional 10 min.

On the Friday immediately following treadmill familiarization, we subjected mice to an exercise capacity test. For this, the mice were acclimated to the treadmill for 10 min, with the speed and incline set initially to zero. The treadmill speed was then increased to 8.5 m/min with an angle of inclination set to 0° for 9 min. Next, the treadmill speed and incline were increased to 10 m/min and 5°, respectively, for 3 min. The speed was then increased by 2.5 m/min every 3 min to a maximum speed of 40 m/min, while inclination increased by 5° every 9 min until a maximum incline of 15° was achieved.

A priori criteria for exercise-induced exhaustion were: 10 consecutive seconds on the electric grid; spending more than 50% of time on the grid; and/or lack of motivation to manual prodding. Each mouse was removed immediately from their respective lane once one or more of these criteria was reached. Blood lactate levels provided a biochemical indicator of exercise-induced exhaustion at or near maximal oxygen consumption (VO_2max).[4-7] We recorded lactate concentration in 0.7 µl of blood from a small tail clip (Lactate Plus meter; Nova Biomedical) prior to the protocol and upon meeting the exhaustion criteria defined above. High lactate levels increase confidence in a successful exercise capacity test by ensuring that failure to continue is due to exhaustion at or near VO_2max and not a failure to comply with the protocol.[8-10]

Following 4 weeks of training, we repeated this testing protocol to assess improvements in exercise capacity. Exercise capacity was measured using the parameters of distance run (meters achieved prior to exhaustion) and work accomplished [calculated as the product of body weight (kg) and vertical distance (m); vertical distance = (distance run)(sinθ), where θ = the angle of inclination of the treadmill from 0°-15°] as outlined previously.[3, 11]

Exercise Training: Mice assigned to exercise training groups were subjected to a 4-week protocol of forced treadmill running. The training protocol commenced the Monday after the initial exercise capacity testing with mice exercising 5 d/wk (Mon–Fri) at 75% of their maximal speed achieved during the initial exercise capacity test and an inclination appropriate to the speed. Prior to each training bout, we provided mice with a "warm-up" period of 10 min at 0 m/min and 10 min at 12 m/min to promote exercise protocol compliance and to minimize risk of injury. In all groups, we progressively increased the workload of the mice, such that they trained for 40 min during week 1, 50 min during week 2, and 60 min during weeks 3 and 4. We chose this progressive intensity protocol to prevent training plateau and to stimulate systemic and cardiac adaptations.[3]

To test the effects of chronic exercise in the adapted and recovery state, mice were euthanized 24 h or 1 h after the last training session of the 4 wk training regimen, respectively. To interrogate the effects of an acute, single-bout of exercise on cardiac metabolism, mice were subjected to familiarization as previously outlined and euthanized immediately following the completion of a 1 d, single exercise training session; 40 min at 75% intensity. Mice were excluded from the study if they were non-compliant with the exercise protocol or if they were found to be injured or in poor health, e.g., due to fighting, etc.

Echocardiographic Assessment: Transthoracic echocardiography of the left ventricle was performed as previously described.[12, 13] Measurements were made on the Vevo 770 echocardiography instrument. Body temperature was maintained (36.5–37.5°C) using a rectal thermometer interfaced with a servo-controlled heat lamp. Mice were anesthetized with 2% isoflurane, maintained under anesthesia with 1.5% isoflurane, and examined. Using short-axis B-modes and endocardial values, stroke volume (SV) was calculated as: diastolic volume – systolic

volume; ejection fraction (EF%) as SV/diastolic volume × 100%; cardiac output as SV × heart rate (HR). Left ventricular diameters during diastole (LVIDd), left ventricular diameters during systole (LVIDs), and heart rate were determined from long-axis M-modes. Relative wall thickness was calculated as (diastolic posterior wall thickness + diastolic anterior wall thickness)/LVIDd. To prevent bias, the individuals performing echocardiography and image tracing were unaware of the group assignments.

Radiometric measurement of myocardial glucose utilization: Hearts were excised and perfused in non-recirculating Langendorff mode with Krebs-Henseleit (KH) buffer (37ºC; 5% CO_2/95% O_2; containing in mmol/L: 118.5 NaCl, 25 $NaHCO_3$, 4.7 KCl, 1.2 $MgSO_4$, 1.2 KH_2PO_4, 2.5 $CaCl_2$ and 5 mM glucose; pH 7.4). Glycolytic flux was assessed by measuring the amount of ^3H_2O released through the metabolism of exogenous [5-^{3}H]glucose (Perkin Elmer), as previously described.[1, 2] Briefly, following a 20 min period of perfusion (equilibration), KH buffer containing 25 µCi/ml of [5-^{3}H]glucose was infused into the cannula via a syringe infusion pump (Harvard Apparatus) at a proportion 1:100 to that of the flow rate (final concentration = 0.25 µCi/ml). The perfusate was collected in two separate 5-min intervals. From the collected perfusate, 400 µl of perfusate was added to 25 µl of 0.6 M HCl in a microcentrifuge tube. The microcentrifuge tube was then placed in a scintillation vial containing 2 ml of H_2O to allow for evaporation diffusion of $[^3H]_2O$ in the microcentrifuge tubes into the water contained in the scintillation vial. To account for incomplete equilibration of $[^3H]_2O$, in parallel vials, known amounts (µCi) of [5-^{3}H]glucose and $[^3H]_2O$ (Moravek Biochemicals) were placed in microcentrifuge tubes, and placed into separate scintillation vials containing 0.5 ml dH_2O. After 72 h incubation at 37°C, the microcentrifuge tube was removed from the vial, 10 ml of scintillation fluid was added, and scintillation counting was performed using a Tri-Carb 2900TR Liquid Scintillation Analyzer (Packard Bioscience Company). Glucose utilization was then calculated using the formula reported by Ashcroft,[14] with considerations for: the specific activity of [5-^{3}H]glucose; incomplete equilibration and background; the dilution of [5-^{3}H]- to unlabeled-glucose; and scintillation counter efficiency. Glucose utilization was normalized to total heart weight and represented as a fold change to the control group. To prevent bias, the individual assisting in hanging the hearts for perfusion was unaware of the group assignments.

Measurement of blood glucose and lactate: Blood lactate concentration was measured in 0.7 µl of blood from a small tail clip using a Lactate Plus meter (Nova Biomedical). Blood glucose concentration was measured from the same tail clip using the Accu-Check Aviva blood glucose monitoring meter (Roche).

Assessment of plasma free fatty acids: Circulating plasma free fatty acids (FFA) were assessed via a colorimetric enzymatic assay, per manufacturers guidelines (Sigma-Aldrich). Briefly, plasma was incubated with acyl-CoA synthetase for 30 min at 37ºC, in a 96-well microplate. A master reaction mix was added to each well and samples were again incubated for 30 min at 37ºC. Absorbance was then measured at 570 nm wavelength and the concentration of FFA in each sample was calculated based on a standard curve.

Measurement of plasma IGF-1: Plasma IGF-1 was quantified using a mouse/rat IGF-1 quantikine ELISA kit (R&D Systems, Minneapolis, MN). Briefly, plasma was diluted 500-fold, added to microplate, and incubated for 2 h at room temperature with constant shaking. The microplate was then washed 5× followed by addition of secondary antibody and incubation at room temperature for 2 h with constant shaking. The microplate was then washed five times. For colorimetric

determination, substrate solution was added to each well for 30 min, followed by addition of stop solution and determination of color intensity by measuring at 450 nm with wavelength correction at 540 nm. The concentration of IGF-1 was calculated using a standard curve.

Mitochondrial function: Heart mitochondria were isolated and subjected to respiratory function assays using the Seahorse XF24, similar to that described previously.[15] Briefly, whole hearts were washed 5× with cold buffer A (220 mM mannitol, 70 mM sucrose, 5 mM MOPS, 1 mM EDTA; pH 7.2 with KOH) followed by homogenization using a glass-col homogenizer in 2 ml of buffer A containing 0.2% fatty acid-free BSA. Homogenate was then subjected to centrifugation at 800*g* for 10 min followed by supernatant collection and centrifugation at 10,000*g* for 10 min. The pellet containing mitochondria was then resuspended in 1 ml fresh buffer A (without BSA) and centrifuged at 10,000*g*, with this step repeated once. The washed mitochondrial pellet was then resuspended in 150 µl respiration buffer (120 mM KCl, 25 mM Sucrose, 10 mM HEPES, 1 mM $MgCl_2$, 5 mM KH_2PO_4; pH 7.2 with KOH) and kept on ice.

To determine mitochondrial function, samples were diluted to a concentration of 5 µg (protein) in 50 µl respiration buffer per well, and centrifuged onto XF24 microplates at 500*g* for 3 min at 4ºC. State 3 respiration in response to substrates were measured after injection of pyruvate + malate (5.0 mM + 2.5 mM, final concentrations), succinate + rotenone (10 mM + 1 µM, final concentrations), or palmitoylcarnitine + malate (50 µM + 0.5 mM, final concentrations). The oxygen consumption rates recorded after injection of oligomycin (1 µg/ml), an inhibitor of ATP synthase, served as a measure of State 4 respiration. Respiratory control ratios, state 3/state 4, was calculated as a measure of the coupling of oxygen consumption to ATP production.

Measurement of F-2,6-P_2 metabolite concentration: Metabolite levels of F-2,6-P_2 were measured in isolated cardiac myocytes as outlined previously.[1, 2]

Glycogen Assay: To assess myocardial glycogen content, 15 mg of heart tissue powder was added to 100 µl of ice-cold dH_2O, homogenized using a glass col homogenizer, boiled for 10 min, and centrifuged at 16,000*g* for 10 min. Glycogen was then hydrolyzed in a 384-well plate for 1 h at 37°C followed by addition of reaction mix containing the OxiRed probe for 1 h at 37°C. Absorbance was then measured at 590 nm. The amount of glycogen was determined against a standard curve and normalized to tissue wet weight.

Histology: Following euthanasia, the heart tissue was excised, flushed with 1 M KCl solution, and fixed in 10% formalin, embedded in paraffin, and sectioned at 4 µm. Heart cross-sections were stained with 4'6-diamidino-2-phenylindole (DAPI; Invitrogen, Carlsbad, CA) and wheat germ agglutinin (WGA; ThermoFisher, Waltham, MA) for quantification of cardiomyocyte cross-sectional area. Additionally, sections were stained with isolectin B4 (Vector Laboratories, Burlingame, CA) to assess capillary density and sirius red for fibrosis. Quantitative measurements were determined using Nikon Elements software, with no less than 100 myocytes with centrally located nuclei assessed for area measurements. To prevent bias, the individual analyzing all histology was unaware of the group assignments. A subset of slides from each group was used based on power calculations to detect a 20% difference in cross-sectional area and capillary:myocyte ratio at $\alpha < 0.05$.

Protein and mRNA Expression Analysis: For measuring protein abundance, tissues and cells were homogenized in buffer containing 50 mM HEPES (pH 7.0), 2 mM EDTA, 1% NP-40, 10% glycerol, 1 mM $MgCl_2$, 1 mM $CaCl_2$, and 150 mM NaCl; fresh phosphatase and protease inhibitors

were added immediately prior to tissue homogenization. The homogenates were sonicated on ice and centrifuged at 13,000*g* for 20 min. Proteins in the supernatant were separated by SDS-PAGE, electroblotted to PVDF membranes, and probed according to the manufacturers' protocols. A horseradish peroxidase-linked secondary antibody (Cell Signaling Technology, Danvers, MA) was used to detect immunoreactive proteins. Images were recorded using a Fujifilm LAS-300 imager, and relative protein abundance was measured via densitometric analysis using TotalLab software.

For transcriptional expression analysis via RT-PCR, RNA was extracted from tissues and cells using the RNeasy Plus Universal Kit (Qiagen, Germantown, MD), followed by cDNA synthesis. Real-time PCR amplification was performed with SYBR Green quantitative PCR (qPCR) Master Mix (SA Biosciences, Germantown, MD) using a 7900HT Fast Real-Time PCR System (Applied Biosystems, Foster, CA). Relative expression was determined by the $2^{-\Delta\Delta Ct}$ method. A list of the antibodies and primers used can be found below.

Antibodies used in these studies.

Antibodies	SOURCE	IDENTIFIER
DAPI (4',6-Diamidino-2-Phenylindole, Dihydrochloride)	ThermoFisher	Cat#D1306
WGA (Wheat germ agglutinin, Alexa Fluor 647 conjugate)	ThermoFisher	Cat#W32466
Fluorescein labeled griffonia simplicifolia lectin I (GSL I) isolectin B4	Vector Laboratories	Cat#FL-1201
Sirius Red	Sigma-Aldrich	Cat#365548
Rabbit monoclonal anti-p-Akt (S473)	Cell Signaling Technology	Cat#4060
Rabbit polyclonal anti-Akt	Cell Signaling Technology	Cat#9272
Rabbit monoclonal anti-p-PFK2 (S483;PFKFB2)	Cell Signaling Technology	Cat#13064
Rabbit polyclonal anti-PFK2 (PFKFB2; heart isoform)	Bethyl Labs	Cat#A304-286A-M
Rabbit monoclonal anti-HK1	Cell Signaling Technology	Cat#2024
Rabbit monoclonal anti-HK2	Cell Signaling Technology	Cat#2867
Rabbit polyclonal anti-PFK1	Santa Cruz Biotechnology	Cat#sc-67028
Rabbit polyclonal anti-PFK2 (PFKFB1; liver isoform)	Novus Biologicals	Cat#NB100-92391
Rabbit polyclonal anti-PFK2 (PFKFB3; ubiquitous isoform)	Proteintech	Cat#13763-1-AP
Rabbit monoclonal anti-PKM1/2	Cell Signaling Technology	Cat#3106
Rabbit polyclonal anti-GFAT1	Santa Cruz Biotechnology	Cat#sc-134894
Rabbit polyclonal anti-GS	Cell Signaling Technology	Cat#3893
Mouse monoclonal anti-LDHB	Abcam	Cat#ab85319

PCR primers used in these studies.

Sequence-Based Reagents		
Gene of Interest	**Forward**	**Reverse**
Cited4 primers	CATGGACACCGAGCTCATC	CTGACCCCAGGTCTGAGAAG

Cebpb primers	GGGGTTGTTGATGTTTTGGT	TCGAAACGGAAAAGGTTCTCA
Nfatc2 primers	CACAGATACGGTGACCCCT	GTGGGATCGGGTTCTTCTTC
HPRT	AGGACCTCTCGAAGTGTTGG	AGGGCATATCCAACAACAAAC

Analysis of cardiac ultrastructure: Transmission electron microscopy analysis, left ventricular tissue was dissected into 3 mm^3 pieces and fixed in 2.5% glutaraldehyde overnight. The samples were then post-fixed in 2% aqueous osmium tetroxide, dehydrated in ascending concentrations of ethanol and embedded in Araldite 502 (Electron Microscopy Sciences, Hatfield PA). One-micron thick sections were stained with toluidine blue for screening under a light microscope. Selected blocks in which the muscle had a longitudinal orientation were cut into 800 Å thick sections, mounted on 200-mesh copper grids, doubly stained with uranyl acetate and lead citrate, and examined in a Phillips CM-10 electron microscope with a LaB 6 cathode (Phillips Electronic Instruments Co., New York, NY) operating at 80 kV.

Metabolomic Analysis: Hearts were freeze-clamped *in situ* using liquid nitrogen-cooled Wollenberger Tongs, which helps to capture the metabolome as it is in the beating mouse heart i*n vivo*. Samples were prepared by Metabolon using their automated MicroLab STAR® system (Hamilton Company, Reno, NV). First, tissue homogenates were made in water at a ratio of 5 uL per mg of tissue. For quality control, several recovery standards were added prior to the first step in the extraction process. To remove protein, dissociate small molecules bound to protein or trapped in the precipitated protein matrix, and to recover chemically diverse metabolites, proteins were then precipitated with methanol (final concentration 80% v/v) under vigorous shaking for 2 min (Glen Mills GenoGrinder 2000) followed by centrifugation. For quality assurance and control, a pooled matrix sample was generated by taking a small volume of each experimental sample to serve as a technical replicate throughout the data set. Extracted water samples served as process blanks. A cocktail of standards known not to interfere with the measurement of endogenous compounds was spiked into every analyzed sample, allowing instrument performance monitoring and aiding chromatographic alignment.

The extract was divided into fractions for analysis by reverse phase (RP)/UPLC-MS/MS with positive ion mode electrospray ionization (ESI), by RP/UPLC-MS/MS with negative ion mode ESI, and by HILIC/UPLC-MS/MS with negative ion mode ESI. Samples were placed briefly on a TurboVap® (Zymark) to remove the organic solvent. All methods utilized a Waters ACQUITY UPLC and a Thermo Scientific Q-Exactive high resolution/accurate mass spectrometer interfaced with a heated electrospray ionization (HESI-II) source and Orbitrap mass analyzer operated at 35,000 mass resolution. The sample extract was reconstituted in solvents compatible with each MS/MS method. Each reconstitution solvent contained a series of standards at fixed concentrations to ensure injection and chromatographic consistency. One aliquot was analyzed using acidic positive ion conditions, chromatographically optimized for hydrophilic compounds. In this method, the extract was gradient eluted from a C18 column (Waters UPLC BEH C18-2.1x100 mm, 1.7 µm) using water and methanol, containing 0.05% perfluoropentanoic acid (PFPA) and 0.1% formic acid (FA). For more hydrophobic compounds, the extract was gradient eluted from the aforementioned C18 column using methanol, acetonitrile, water, 0.05% PFPA and 0.01% FA. Aliquots analyzed using basic negative ion optimized conditions were gradient eluted from a separate column using methanol and water, containing 6.5 mM ammonium bicarbonate (pH 8). The last aliquot was analyzed via negative ionization following elution from a HILIC column (Waters UPLC BEH Amide 2.1×150 mm, 1.7 µm) using a gradient consisting of water and

acetonitrile with 10 mM ammonium formate (pH 10.8). The MS analysis alternated between MS and data-dependent MS^n scans using dynamic exclusion. The scan range covered 70–1000 *m/z*.

Raw data were extracted, peak-identified and processed using Metabolon's proprietary hardware and software. Compounds were identified by comparison to library entries of purified, authenticated standards or recurrent unknown entities, with known retention times/indices (RI), mass to charge ratios (*m/z*), and chromatographic signatures (including MS/MS spectral data). Biochemical identifications were based on three criteria: retention index within a narrow RI window of the proposed identification, accurate mass match to the library±10 ppm, and the MS/MS forward and reverse scores between experimental data and authentic standards. Proprietary visualization and interpretation software (Metabolon, Inc., Durham, NC) was used to confirm the consistency of peak identification among the various samples. Library matches for each compound were checked for each sample and corrected, if necessary. Area under the curve was used for peak quantification.

Original scale data (raw area counts) were analyzed using Metaboanalyst 3.0 software (http://www.metaboanalyst.ca/).[16] Metabolites with greater than 50% of the values missing were omitted from the analysis, and missing values were imputed by introducing values with half the minimum positive value in the original data. An interquartile range filter was used to identify and remove variables unlikely to be of use when modeling the data. The data were log-transformed and auto-scaled (mean-centered and divided by the standard deviation of each variable). Univariate (e.g., volcano plots) and multivariate (e.g., PCA) analyses were then performed. For multiple comparison testing, *q* values were calculated as in R using a method embedded within the Metaboanalyst software, controlling for the false discovery rate.[17] Radar charts were constructed in R using average Z-scores of significantly different metabolites from each biochemical pathway.

Transcriptomic analyses: Hearts of male WT, $Glyco^{Lo}$ and $Glyco^{Hi}$ mice (15–16 weeks of age) were subjected to transcriptomic analysis using the GeneChip® Mouse Genome 430 2.0 Array (Affymetrix, Inc.). Array data were analyzed using the affy[18] and limma[19] packages of R for Robust Multi-array Average (RMA) for normalization and for moderate t-statistics to derive p-values, respectively. The p-values were adjusted using the Benjamini and Hochberg method for false discovery rate control.[17] For the genes with multiple probe set IDs, the probe set with the highest standard deviation among all samples was kept for further analysis. Gene Ontology analysis was performed using DAVID (https://david.ncifcrf.gov/home.jsp).[20]

Data and Software Availability: Cytoscape software was used to visualize changes in metabolic pathways and networks and was facilitated using the MetaboLync Cytoscape Plugin (Metabolon, Inc). Metabolomic data were analyzed using Metaboanalyst 3.0 software. Gene array data has been deposited in the Gene Expression Omnibus databank (GSE100176) and will be made available to readers upon publication.

Statistical analysis: Statistical parameters including the value of n (number of mice), the definition of center, dispersion and precision measures (mean ± SEM or SD) and statistical significance are reported in the Figures and Figure Legends. A p value of ≤ 0.05 was considered statistically significant. In the Figures, asterisks denote statistical significance as calculated by unpaired or paired Student's t test (for direct comparisons); Levene's test was used to assess the equality of group variances between groups, and if found to be significantly different, a Welch-modified t-test was used to assess significance. Multiple comparisons were assessed by one-way or two-way ANOVA followed by Bonferroni or Sidak Multiple Comparison tests (*, $p<0.05$; **, $p<0.01$; ***,

p<0.001; ****, p<0.0001), as appropriate. Statistical analysis was performed using GraphPad Prism 7, Metaboanalyst, and/or the R program.

B. Supplementary References

1. Donthi RV, Ye G, Wu C, McClain DA, Lange AJ and Epstein PN. Cardiac expression of kinase-deficient 6-phosphofructo-2-kinase/fructose-2,6-bisphosphatase inhibits glycolysis, promotes hypertrophy, impairs myocyte function, and reduces insulin sensitivity. *J Biol Chem*. 2004;279:48085-90.
2. Wang Q, Donthi RV, Wang J, Lange AJ, Watson LJ, Jones SP and Epstein PN. Cardiac phosphatase-deficient 6-phosphofructo-2-kinase/fructose-2,6-bisphosphatase increases glycolysis, hypertrophy, and myocyte resistance to hypoxia. *Am J Physiol Heart Circ Physiol*. 2008;294:H2889-97.
3. Gibb AA, McNally LA, Riggs DW, Conklin DJ, Bhatnagar A and Hill BG. FVB/NJ Mice Are a Useful Model for Examining Cardiac Adaptations to Treadmill Exercise *Frontiers in Physiology* 2016;7:636.
4. McConnell TR. Practical considerations in the testing of VO2max in runners. *Sports Med*. 1988;5:57-68.
5. Ferreira JC, Rolim NP, Bartholomeu JB, Gobatto CA, Kokubun E and Brum PC. Maximal lactate steady state in running mice: effect of exercise training. *Clin Exp Pharmacol Physiol*. 2007;34:760-5.
6. Hakimi P, Yang J, Casadesus G, Massillon D, Tolentino-Silva F, Nye CK, Cabrera ME, Hagen DR, Utter CB, Baghdy Y, Johnson DH, Wilson DL, Kirwan JP, Kalhan SC and Hanson RW. Overexpression of the cytosolic form of phosphoenolpyruvate carboxykinase (GTP) in skeletal muscle repatterns energy metabolism in the mouse. *The Journal of biological chemistry*. 2007;282:32844-55.
7. Pederson BA, Cope CR, Schroeder JM, Smith MW, Irimia JM, Thurberg BL, DePaoli-Roach AA and Roach PJ. Exercise capacity of mice genetically lacking muscle glycogen synthase: in mice, muscle glycogen is not essential for exercise. *The Journal of biological chemistry*. 2005;280:17260-5.
8. Billat VL, Mouisel E, Roblot N and Melki J. Inter- and intrastrain variation in mouse critical running speed. *J Appl Physiol (1985)*. 2005;98:1258-63.
9. Von Wittke P, Lindner A, Deegen E and Sommer H. Effects of training on blood lactate-running speed relationship in thoroughbred racehorses. *J Appl Physiol (1985)*. 1994;77:298-302.
10. Gladden LB. Lactate metabolism: a new paradigm for the third millennium. *J Physiol*. 2004;558:5-30.
11. Massett MP and Berk BC. Strain-dependent differences in responses to exercise training in inbred and hybrid mice. *American journal of physiology Regulatory, integrative and comparative physiology*. 2005;288:R1006-13.
12. Sansbury BE, DeMartino AM, Xie Z, Brooks AC, Brainard RE, Watson LJ, DeFilippis AP, Cummins TD, Harbeson MA, Brittian KR, Prabhu SD, Bhatnagar A, Jones SP and Hill BG. Metabolomic analysis of pressure-overloaded and infarcted mouse hearts. *Circulation Heart failure*. 2014;7:634-42.
13. Watson LJ, Facundo HT, Ngoh GA, Ameen M, Brainard RE, Lemma KM, Long BW, Prabhu SD, Xuan YT and Jones SP. O-linked beta-N-acetylglucosamine transferase is indispensable in the failing heart. *Proc Natl Acad Sci U S A*. 2010;107:17797-802.
14. Ashcroft SJ, Weerasinghe LC, Bassett JM and Randle PJ. The pentose cycle and insulin release in mouse pancreatic islets. *Biochem J*. 1972;126:525-32.

15. Sato S, Ogura Y, Mishra V, Shin J, Bhatnagar S, Hill BG and Kumar A. TWEAK promotes exercise intolerance by decreasing skeletal muscle oxidative phosphorylation capacity. *Skeletal muscle*. 2013;3:18.
16. Xia J, Sinelnikov IV, Han B and Wishart DS. MetaboAnalyst 3.0--making metabolomics more meaningful. *Nucleic acids research*. 2015;43:W251-7.
17. Benjamini Y and Hochberg Y. Controlling the false discovery rate: a practical and powerful approach to multiple testing. *Journal of the Royal Statistical Society Series*. 1995;B57.
18. Gautier L, Cope L, Bolstad BM and Irizarry RA. affy--analysis of Affymetrix GeneChip data at the probe level. *Bioinformatics (Oxford, England)*. 2004;20:307-15.
19. Ritchie ME, Phipson B, Wu D, Hu Y, Law CW, Shi W and Smyth GK. limma powers differential expression analyses for RNA-sequencing and microarray studies. *Nucleic acids research*. 2015;43:e47.
20. Huang da W, Sherman BT and Lempicki RA. Systematic and integrative analysis of large gene lists using DAVID bioinformatics resources. *Nat Protoc*. 2009;4:44-57.

C. Supplemental Figures

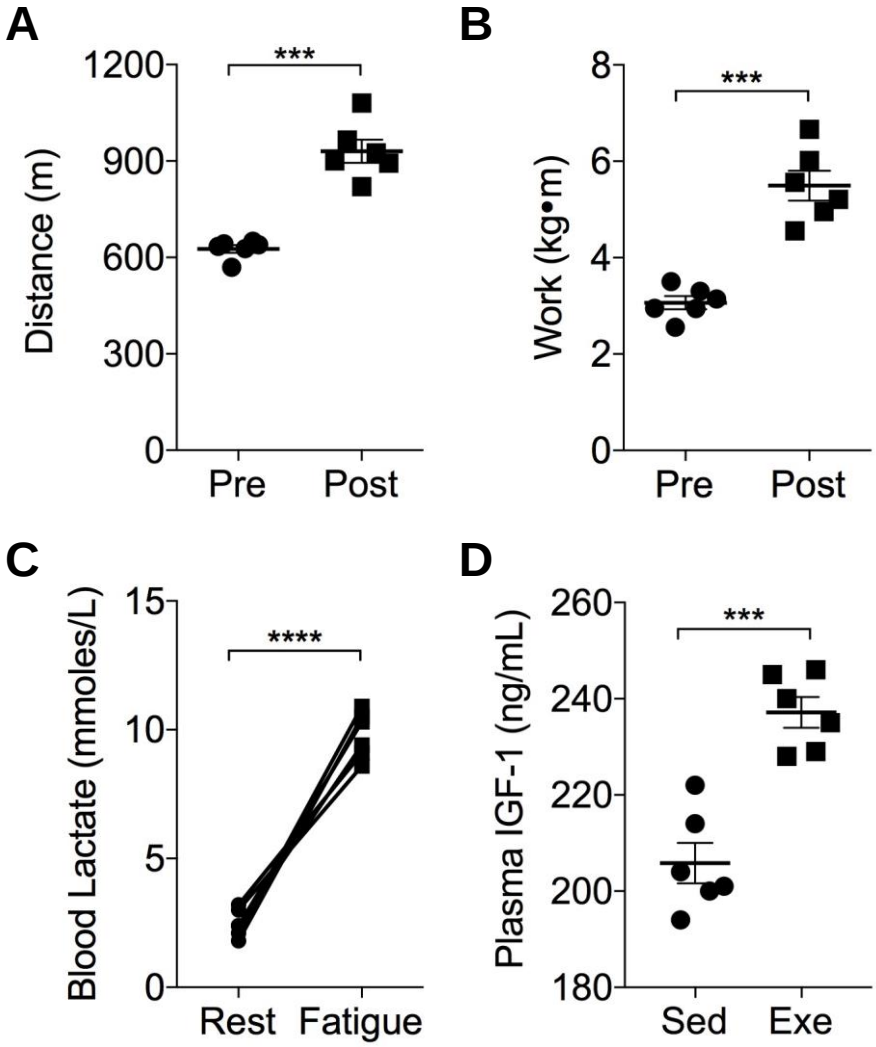

Fig S1. Exercise training improves exercise capacity. Systemic adaptation to a 4-wk treadmill training protocol: Pre- and post-training (**A**) distance and (**B**) work; (**C**) Validation of a successful high-intensity exercise capacity test as indicated by levels of blood lactate measured at rest and immediately after the criteria for exercise-induced fatigue were met; and (**D**) Plasma levels of insulin-like growth factor-1 (IGF-1). Sed, sedentary; Exe, exercise. Data represented as mean ± SEM; ***$p < 0.001$, ****$p < 0.0001$; n = 6 per group

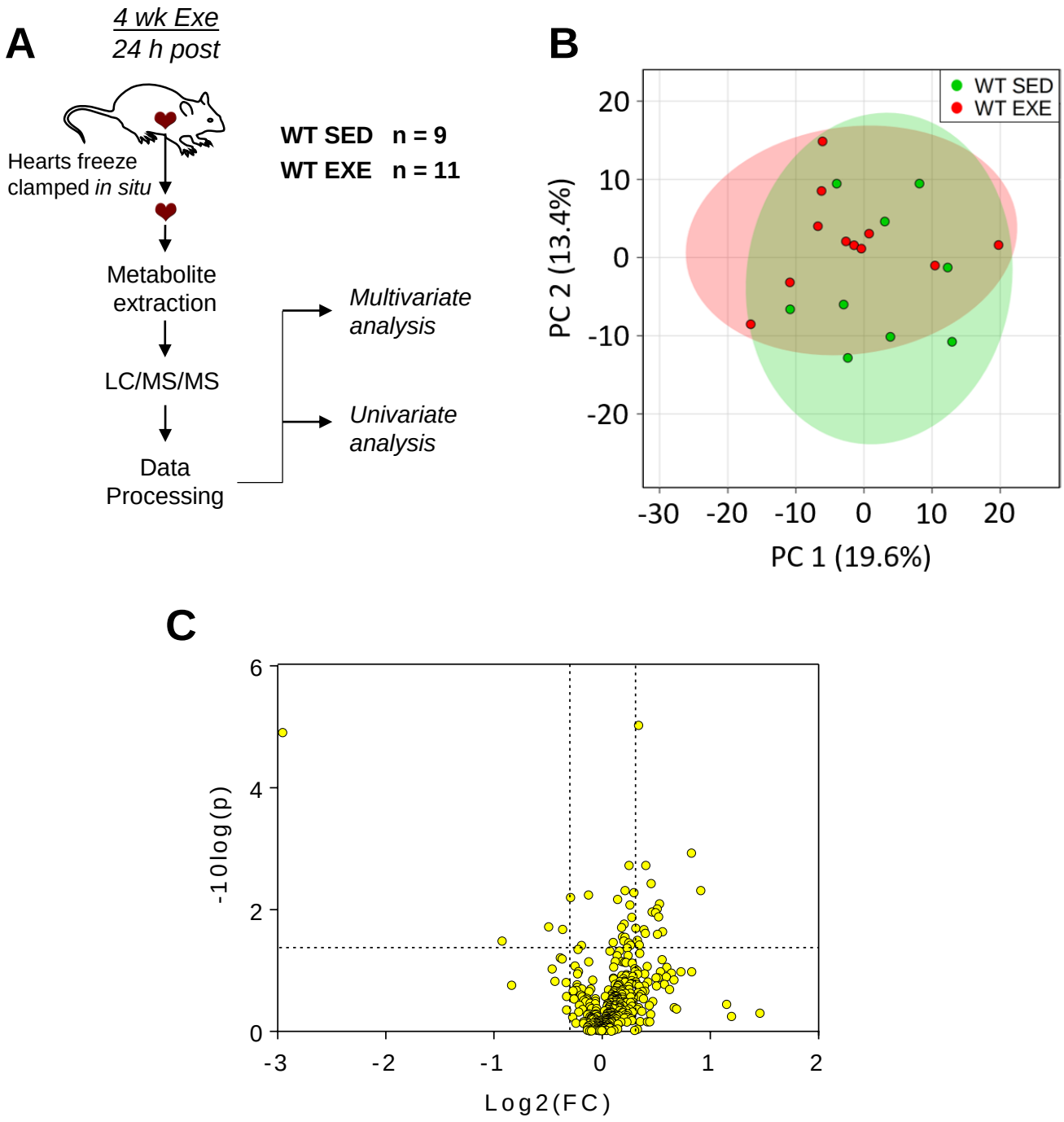

Fig S2. Metabolomic changes in the exercise-adapted mouse heart. (**A**) Mice were either exercised for 4-wk (EXE) or remained sedentary (SED) under similar handling conditions. Following a 6 h fast and 24 h after the final exercise session, hearts were freeze-clamped *in situ*. The relative abundance of metabolites in the hearts was examined by LC/MS/MS; (**B**) 2D PCA analysis; (**C**) Volcano plot showing metabolites that changed ≥ 1.25-fold ($p \leq 0.05$) in Exe hearts compared with Sed hearts. A list of metabolites found to be significantly different in exercise-adapted hearts can be found in Table S2. n = 9 Sed and 11 Exe mouse hearts per group.

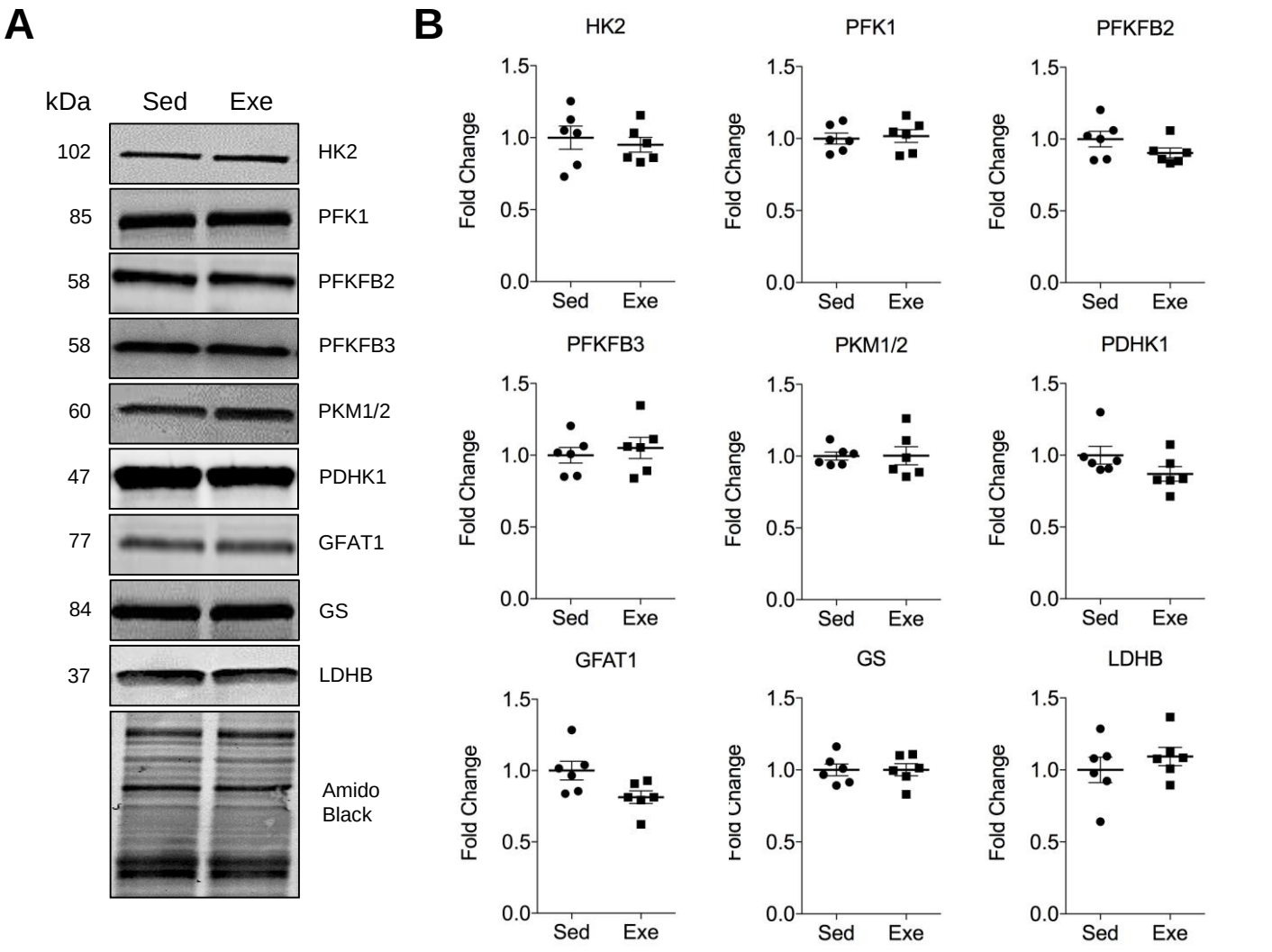

Fig S3. Exercise training does not alter the abundance of key glucose-metabolizing enzymes. Western blot analysis of enzymes in glycolysis and glucose metabolism: (**A**) Representative western blots of hexokinase 2 (HK2), phosphofructokinase (PFK1), phosphofructo-kinase/fructose-bisphosphatase 2 (PFKFB2; PFK2), phosphofructo-kinase/fructose-bisphosphatase 3 (PFKFB3; PFK2), pyruvate kinase (PKM1/2), pyruvate dehydrogenase kinase 1 (PDHK1), glutamine:fructose-6-phosphate aminotransferase 1 (GFAT1), glycogen synthase (GS), and lactate dehydrogenase b (LDHB); (**B**) Quantification of western blots from A. Data are represented as mean ± SEM; n = 6 per group; in all cases, $p>0.05$ after Bonferroni correction.

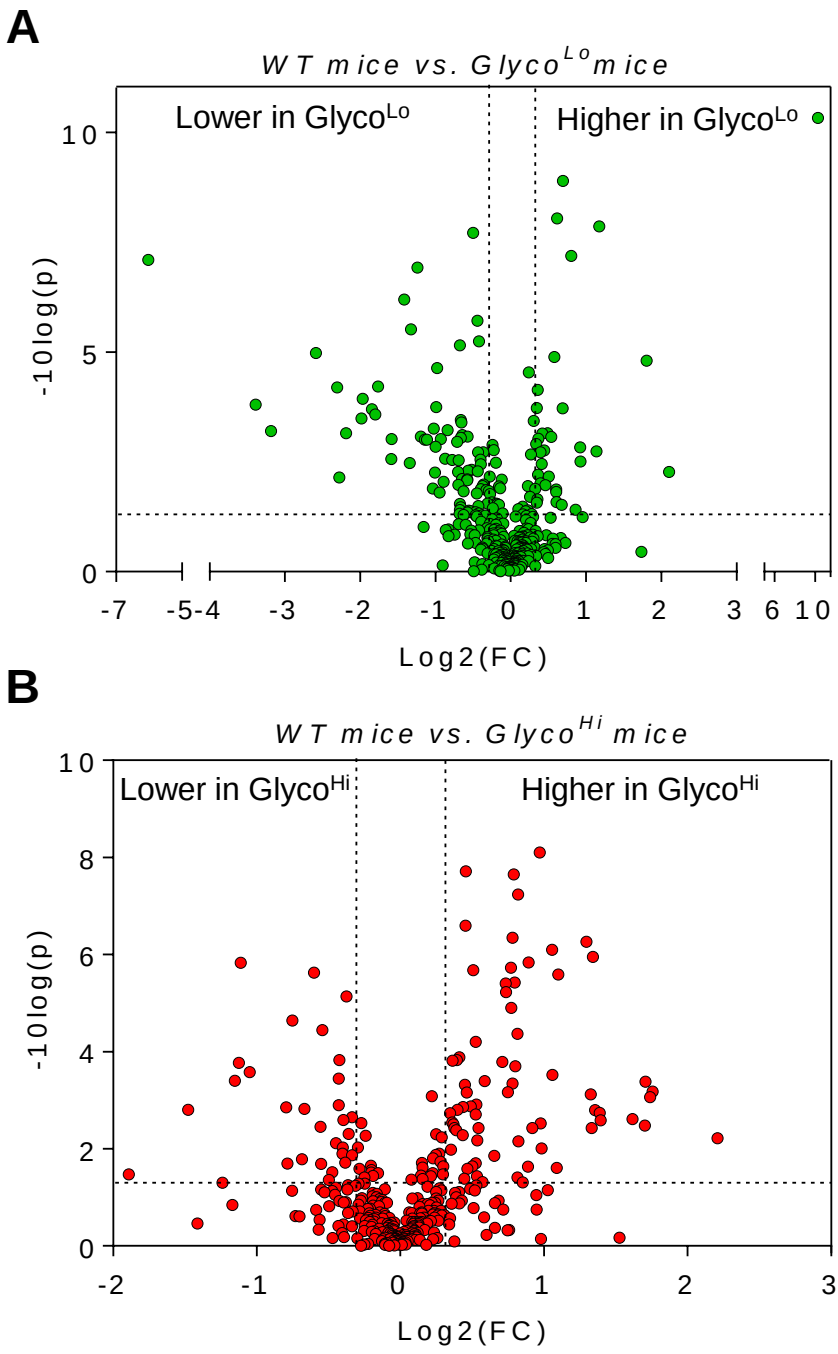

Fig S4. Metabolomic changes in the Glyco^{Lo} and Glyco^{Hi} mouse hearts. Following a 6 h fast, hearts were freeze-clamped *in situ*. The relative abundance of metabolites in the hearts was measured by LC/MS/MS. Volcano plot showing metabolites that changed ≥ 1.25-fold ($p \leq 0.05$) in (**A**) Glyco^{Lo} and (**B**) Glyco^{Hi} hearts compared with WT hearts; A list of metabolites found to be significantly different in these hearts can be found in Tables S3 and S4. n = 9 WT, 10 Glyco^{Lo}, 10 Glyco^{Hi} mouse hearts per group.

Fig. S5

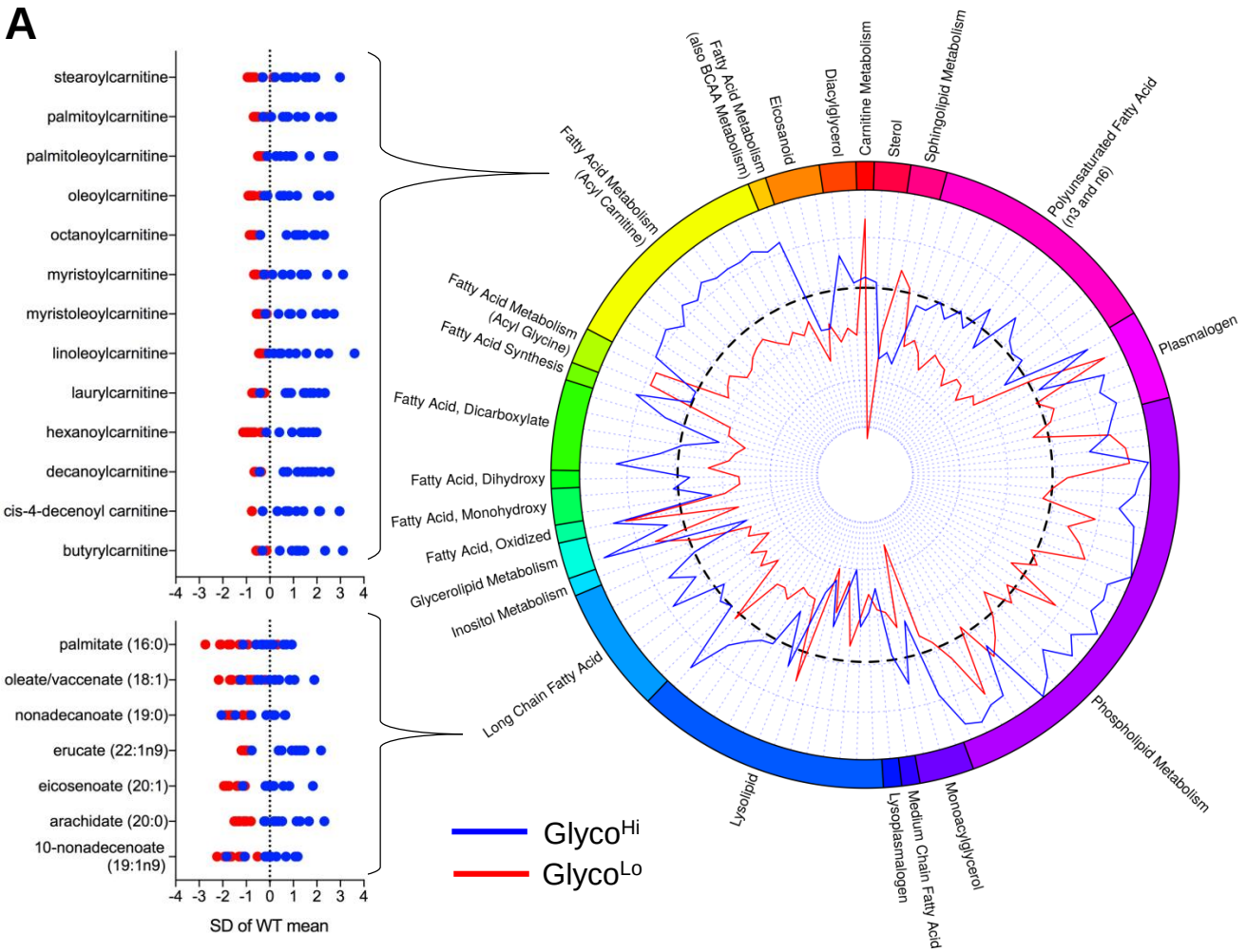
A
stearoylcarnitine
palmitoylcarnitine
palmitoleoylcarnitine
oleoylcarnitine
octanoylcarnitine
myristoylcarnitine
myristoleoylcarnitine
linoleoylcarnitine
laurylcarnitine
hexanoylcarnitine
decanoylcarnitine
cis-4-decenoyl carnitine
butyrylcarnitine
palmitate (16:0)
oleate/vaccenate (18:1)
nonadecanoate (19:0)
erucate (22:1n9)
eicosenoate (20:1)
arachidate (20:0)
10-nonadecenoate (19:1n9)
-4 -3 -2 -1 0 1 2 3 4
SD of WT mean
Fatty Acid Metabolism (Acyl Carnitine)
Fatty Acid Metabolism (also BCAA Metabolism)
Eicosanoid
Diacylglycerol
Carnitine Metabolism
Sterol
Sphingolipid Metabolism
Polyunsaturated Fatty Acid (n3 and n6)
Plasmalogen
Phospholipid Metabolism
Monoacylglycerol
Medium Chain Fatty Acid
Lysoplasmalogen
Lysolipid
Long Chain Fatty Acid
Inositol Metabolism
Glycerolipid Metabolism
Fatty Acid, Oxidized
Fatty Acid, Monohydroxy
Fatty Acid, Dihydroxy
Fatty Acid, Dicarboxylate
Fatty Acid Synthesis
Fatty Acid Metabolism (Acyl Glycine)
GlycoHi
GlycoLo

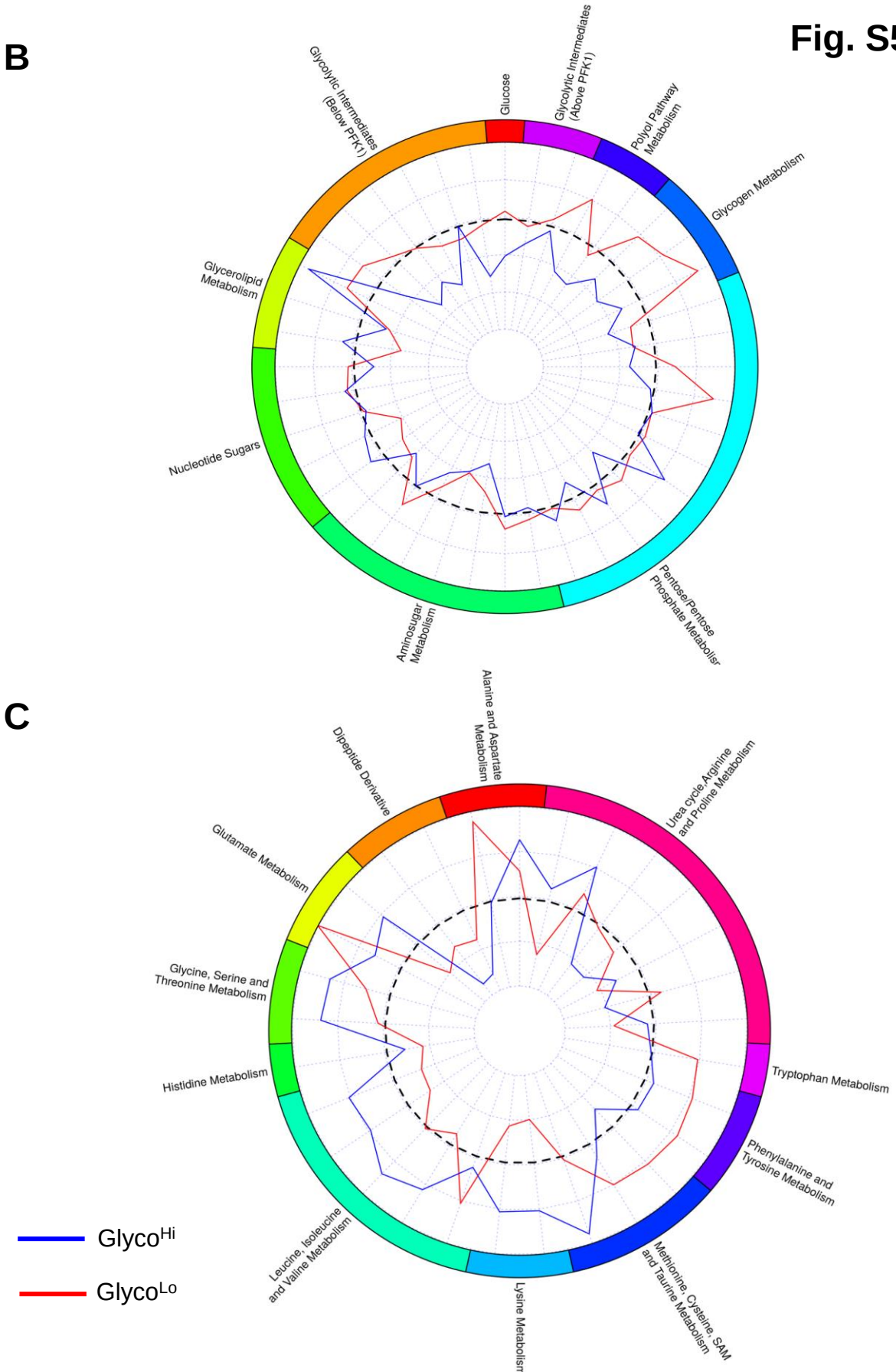

Fig S5. Modulation of cardiac glycolytic rate regulates lipid, carbohydrate, and amino acid metabolism. Spider charts showing average z-scores of (**A**) lipid (**B**) carbohydrate and (**C**) amino acid and peptide metabolites that were significantly different in Glyco^{Lo} or Glyco^{Hi} hearts compared with WT controls. n = 9 WT, 10 Glyco^{Lo}, 10 Glyco^{Hi} mouse hearts per group.

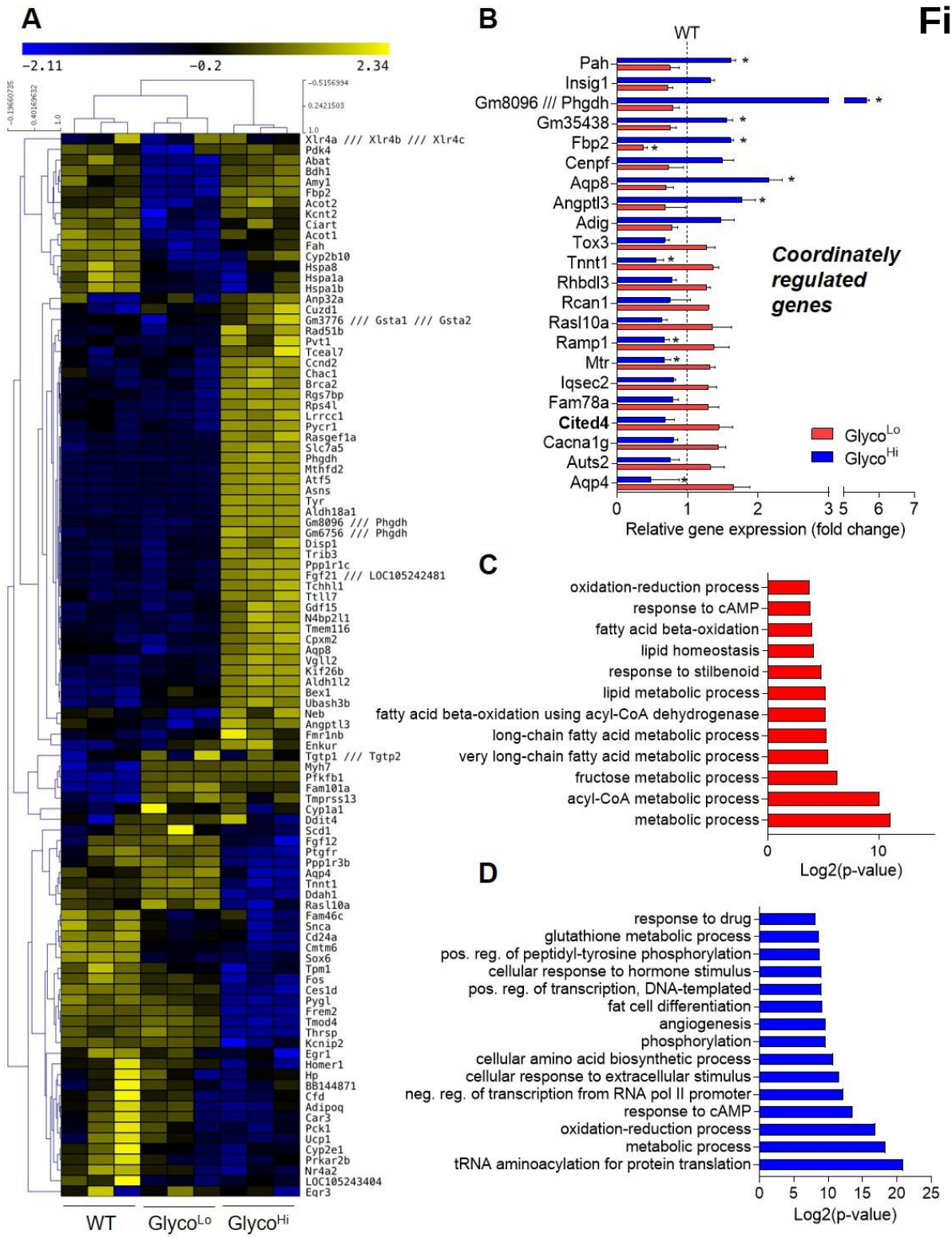

Fig. S6. Myocardial glycolysis coordinately regulates gene transcription in the heart. Results of transcriptomic analyses: (**A**) Robust Multi-array Average (RMA) analysis of top 100 genes that were found to be the most different based on the standard deviation across the samples; (**B**) Genes found to be coordinately regulated by glycolysis: Bars indicate genes with fold-changes at least 1.25-fold lower or higher in PFK2 mutant mice compared with WT controls. All genes shown were significantly different between Glyco^{Lo} and Glyco^{Hi} mice at $p<0.05$, after adjustment for the false discovery rate. Significant differences from the WT controls (dotted line) using the same statistical analysis is shown by the asterisks (*FDR-adjusted p-value<0.05); (**C**) Gene ontology analysis of processes significantly regulated by low rates of glycolysis; and (**D**) Gene ontology analysis of processes significantly regulated by high rates of glycolysis. The 15 most significant processes are shown. n = 3 per group.

D. Supplemental Tables

Table S1: Echocardiographic data from sedentary and exercised WT mice.

	WT-Sed			WT-Exe		
	Mean		SD	Mean		SD
HR (bpm)	482	±	32	492	±	25
Endocardial Values						
EDV (μl)	38	±	3	45	±	6**
ESV (μl)	11	±	3	13	±	2
SV (μl)	27	±	3	32	±	5**
EF (%)	71	±	7	72	±	4
CO (ml/min)	13	±	2	16	±	2**
Chamber Diameter						
LVIDd (mm)	3.7	±	0.2	4.0	±	0.2**
LVIDs (mm)	2.2	±	0.2	2.5	±	0.2**
Wall Thickness						
LVPWd (mm)	0.8	±	0.1	0.9	±	0.1*
LVPWs (mm)	1.2	±	0.1	1.3	±	0.1*
LVAWd (mm)	0.8	±	0.1	0.8	±	0.1
LVAWs (mm)	1.1	±	0.2	1.1	±	0.2
RWT	0.46	±	0.07	0.42	±	0.07
n	12			10		

After acclimatization and an initial exercise capacity test, male FVB/NJ mice (15 weeks of age) were subjected to exercise training 5 d a week for 4 wk. One day following the final exercise capacity test, the mice were anesthetized and cardiac structure and function were assessed by echocardiography. Abbreviations: Sed, sedentary; Exe, exercised; HR, heart rate; EDV, end-diastolic volume; ESV, end-systolic volume; SV, stroke volume; EF, ejection fraction; CO, cardiac output; LVIDd, left ventricular internal diameter in diastole; LVIDs, left ventricular internal diameter in systole; LVPWd, left ventricular posterior wall in diastole; LVPWs, left ventricular posterior wall in systole; LVAWd, left ventricular anterior wall in diastole; LVAWs, left ventricular anterior wall in systole; RWT, relative wall thickness. *$p<0.05$, **$p<0.01$ vs. Sed.

Table S2: Significantly different metabolites in hearts from exercise-adapted mice.

Metabolite	Identifier (KEGG or HMBD)	Relative Fold Change (EXE/SED)	*p* value	*q* value	Super Pathway	Metabolic Subpathway(s)
hexanoylglycine	HMDB00701	1.88	0.005	0.241	Lipid	Fatty Acid Metabolism(Acyl Glycine)
p-cresol-glucuronide*	HMDB11686	1.77	0.001	0.161	Amino Acid	Phe and Tyr Metabolism
3-hydroxybutyrylcarnitine	HMDB13127	1.47	0.023	0.380	Lipid	Fatty Acid Metabolism (Acyl Carnitine)
3-hydroxylaurate	HMDB00387	1.44	0.008	0.256	Lipid	Fatty Acid, Monohydroxy
2-hydroxyadipate	HMDB00321	1.44	0.013	0.300	Lipid	Fatty Acid, Dicarboxylate
3-hydroxymyristate	-	1.43	0.026	0.389	Lipid	Fatty Acid, Monohydroxy
prolylglycine	HMDB11178	1.42	0.010	0.278	Peptide	Dipeptide
3-hydroxydecanoate	HMDB02203	1.41	0.011	0.282	Lipid	Fatty Acid, Monohydroxy
cytidine-5'-diphosphoethanolamine	HMDB01564	1.38	0.011	0.282	Lipid	Phospholipid Metabolism
oleoylcholine	-	1.37	0.003	0.241	Lipid	Phospholipid Metabolism
galactitol (dulcitol)	HMDB00107	1.32	0.002	0.161	Carbohydrate	Fructose, Mannose and Galactose Metabolism
cytidine 5'-diphosphocholine	HMDB01413	1.32	0.025	0.389	Lipid	Phospholipid Metabolism
N-monomethylarginine	HMDB29416	1.31	0.021	0.363	Amino Acid	Urea cycle; Arg and Pro Metabolism
3-hydroxyoctanoate	HMDB01954	1.27	0.038	0.434	Lipid	Fatty Acid, Monohydroxy
lysine	HMDB00182	1.26	<0.001	0.003	Amino Acid	Lys Metabolism
fumarate	HMDB00134	1.25	0.032	0.422	Energy	TCA Cycle
N-delta-acetylornithine	-	0.78	0.021	0.363	Amino Acid	Urea cycle; Arg and Pro Metabolism
pipecolate	HMDB00070	0.71	0.019	0.363	Amino Acid	Lys Metabolism
4-ethylphenyl sulfate	C13637	0.53	0.033	0.422	Xenobiotics	Benzoate Metabolism
4-vinylphenol sulfate	HMDB04072	0.13	<0.001	0.003	Xenobiotic	Benzoate metabolism

Hearts from WT, exercise-adapted (EXE) mice [(and corresponding WT sedentary controls (SED)] were freeze-clamped *in situ*, 24 h after the final exercise bout. Metabolites extracted from the hearts were subjected to LC/MS analysis. Raw area counts from each identified metabolite were log-transformed, autoscaled, and then subjected to t-test analysis. Missing values were imputed using half the minimum value of observed raw area count data, and metabolites with >50% values missing were omitted from the analysis. Asterisks (*) indicate compounds that were not officially confirmed based on a standard, but whose identity matches the expected exact mass using the UHPLC/MS/MS^2 accurate mass platform. Shown are those metabolites with a *p* value threshold of 0.05 and a fold change threshold of 1.25. n = 9 SED mice and n = 10 EXE mice.

Table S3: Significantly different metabolites in hearts from WT and Glyco^{Lo} mice.

Metabolite	Identifier (KEGG or HMBD)	Relative Fold Change (Glyco^{Lo}/WT)	*p* value	*q* value	Super Pathway	Metabolic Subpathway(s)
#S-methylmethionine	C05319	1228	<0.0001	<0.0001	Amino acid	Met, Cys, SAM, Tau metabolism
maltotriose	HMDB01262	4.29	0.0054	0.0304	Carbohydrate	Glycogen metabolism
ribonate	HMDB00867	3.49	<0.0001	0.0004	Carbohydrate	Pentose metabolism
N-acetylaspartate (NAA)	HMDB00812	2.26	<0.0001	<0.0001	Amino acid	Ala, Asp metabolism
aconitate [cis or trans]	HMDB00072	2.20	0.0018	0.0137	Energy	TCA cycle
p-cresol-glucuronide*	HMDB11686	1.90	0.0031	0.0197	Amino acid	Phe, Tyr metabolism
p-cresol sulfate	HMDB11635	1.89	0.0015	0.0120	Amino acid	Phe, Tyr metabolism
1-linoleoyl-2-arachidonoyl-GPE (18:2/20:4)*	-	1.81	0.0391	0.1349	Lipid	Phospholipid
orotidine	HMDB00788	1.74	<0.0001	<0.0001	Nucleotide	Pyrimidine metabolism, orotate containing
methyl glucopyranoside (alpha + beta)	-	1.61	0.0002	0.0032	Xenobiotic	Food component
1-stearoyl-2-oleoyl-GPC (18:0/18:1)	-	1.61	<0.0001	<0.0001	Lipid	Phospholipid
hexanoylglycine	HMDB00701	1.60	0.0299	0.1094	Lipid	Fatty acid metabolism, acylglycine
glutamate	HMDB00148	1.53	<0.0001	<0.0001	Amino acid	Glutamate metabolism
stachydrine	HMDB04827	1.52	0.0152	0.0632	Xenobiotic	Food component
maltose	HMDB00163	1.52	0.0133	0.0577	Carbohydrate	Glycogen metabolism
kynurenine	HMDB00684	1.52	0.0262	0.1028	Amino acid	Tryptophan metabolism
1-(1-enyl-palmitoyl)-2-oleoyl-GPC (P-16:0/18:1)*	-	1.49	<0.0001	0.0004	Lipid	Plasmalogen
deoxycarnitine	HMDB01161	1.45	0.0009	0.0088	Lipid	Carnitine metabolism
2-methylcitrate/homocitrate	-	1.42	0.0068	0.0367	Energy	TCA cycle
mannitol/sorbitol	HMDB00247	1.40	0.0007	0.0080	Carbohydrate	Fructose, mannose, galactose metabolism
gulonic acid*	-	1.37	0.0107	0.0508	Cofactor/Vitamin	Ascorbate/Alderate metabolism
1-stearoyl-2-arachidonoyl-GPE (18:0/20:4)	-	1.36	0.0017	0.0133	Lipid	Phospholipid
alpha-ketoglutarate	HMDB00208	1.36	0.0017	0.0133	Energy	TCA cycle
1-palmitoyl-2-arachidonoyl-GPE (16:0/20:4)*	HMDB05323	1.34	0.0007	0.0080	Lipid	Phospholipid
N-acetylmethionine	HMDB11745	1.33	0.0035	0.0214	Amino acid	Met, Cys, SAM, Tau metabolism
methylsuccinate	HMDB01844	1.32	0.0098	0.0481	Amino acid	BCAA metabolism
1,2-dioleoyl-GPC (18:1/18:1)*	-	1.32	0.0019	0.0137	Lipid	Phospholipid
1-palmitoyl-2-palmitoleoyl-GPC (16:0/16:1)*	-	1.29	0.0009	0.0088	Lipid	Phospholipid
glycerophosphoglycerol	C03274	1.28	0.0223	0.0885	Lipid	Glycerolipid
nicotinamide ribonucleotide (NMN)	HMDB00229	1.28	<0.0001	0.0015	Cofactor/Vitamin	Nicotinate/Nicotinamide metabolism
1,2-dilinoleoyl-GPE (18:2/18:2)*	-	1.28	0.0062	0.0339	Lipid	Phospholipid
methionine sulfone	-	1.27	0.0269	0.1038	Amino acid	Met, Cys, SAM, Tau metabolism
1-stearoyl-2-oleoyl-GPE (18:0/18:1)	-	1.27	0.0002	0.0032	Lipid	Phospholipid
thiamin monophosphate	HMDB02666	1.26	0.0012	0.0106	Cofactor/Vitamin	Thiamine metabolism
4-hydroxy-2-nonenal	HMDB04362	1.25	0.0131	0.0577	Lipid	Fatty acid, oxidized
beta-hydroxyisovalerate	HMDB00754	0.80	0.0139	0.0594	Amino acid	BCAA metabolism
palmitate (16:0)	HMDB00220	0.78	0.0019	0.0137	Lipid	Long chain fatty acid
N6-carboxyethyllysine	-	0.78	0.0104	0.0506	Amino acid	Lysine metabolism
5-dodecenoate (12:1n7)	HMDB00529	0.77	0.0113	0.0528	Lipid	Medium chain fatty acid

12-HEPE	HMDB10202	0.76	0.0036	0.0216	Lipid	Eicosanoid
azelate (nonanedioate)	HMDB00784	0.76	0.0132	0.0577	Lipid	Fatty acid, dicarboxylate
1-linoleoyl-GPC (18:2)	HMDB10386	0.76	0.0028	0.0187	Lipid	Lysolipid
2-methylmalonyl carnitine	HMDB13133	0.75	<0.0001	0.0002	Lipid	Fatty acid synthesis
oleate/vaccenate (18:1)	-	0.75	0.0132	0.0577	Lipid	Long chain fatty acid
octadecanedioate	HMDB00782	0.74	0.0052	0.0299	Lipid	Fatty acid, dicarboxylate
3-hydroxyoctanoate	HMDB01954	0.74	0.0320	0.1151	Lipid	Fatty acid, monohydroxy
nonadecanoate (19:0)	HMDB00772	0.74	0.0019	0.0137	Lipid	Long chain fatty acid
argininosuccinate	HMDB00052	0.74	0.0474	0.1525	Amino acid	Urea cycle; Arg/Pro metabolism
1-palmitoyl-GPC (16:0)	HMDB10382	0.73	<0.0001	<0.0001	Lipid	Lysolipid
homoarginine	HMDB00670	0.73	0.0166	0.0678	Amino acid	Urea cycle; Arg/Pro metabolism
1-methylimidazoleacetate	HMDB02820	0.72	0.0446	0.1466	Amino acid	Histidine metabolism
succinylcarnitine	-	0.71	<0.0001	<0.0001	Energy	TCA cycle
1-oleoyl-GPG (18:1)*	-	0.70	0.0048	0.0285	Lipid	Lysolipid
1-palmitoyl-2-linoleoyl-glycerol (16:0/18:2)*	-	0.69	0.0424	0.1408	Lipid	Diacylglycerol
arachidonate (20:4n6)	HMDB01043	0.68	0.0050	0.0296	Lipid	Long chain fatty acid
1-palmitoyl-GPE (16:0)	HMDB11503	0.68	0.0407	0.1373	Lipid	Lysolipid
2-hydroxyadipate	HMDB00321	0.67	0.0083	0.0419	Lipid	Fatty acid, dicarboxylate
glycerol	HMDB00131	0.67	0.0008	0.0087	Lipid	Glycerolipid metabolism
1-arachidonoyl-GPI (20:4)*	HMDB61690	0.67	0.0079	0.0407	Lipid	Lysolipid
1-linoleoyl-GPE (18:2)*	HMDB11507	0.67	0.0449	0.1466	Lipid	Lysolipid
15-HETE	HMDB02110	0.65	0.0147	0.0617	Lipid	Eicosanoid
10-nonadecenoate (19:1n9)	HMDB13622	0.64	0.0008	0.0086	Lipid	Long chain fatty acid
linolenate [alpha or gamma; (18:3n3 or 6)]	HMDB03073	0.64	0.0078	0.0407	Lipid	Polyunsaturated fatty acid
1-oleoyl-3-linoleoyl-glycerol (18:1/18:2)	-	0.63	0.0344	0.1217	Lipid	Diacylglycerol
13-HODE + 9-HODE	-	0.63	0.0009	0.0088	Lipid	Fatty acid, monohydroxy
arachidate (20:0)	HMDB02212	0.63	<0.0001	0.0002	Lipid	Long chain fatty acid
1-stearoyl-GPE (18:0)	HMDB11130	0.63	0.0398	0.1364	Lipid	Lysolipid
linoleate (18:2n6)	HMDB00673	0.63	0.0004	0.0053	Lipid	Polyunsaturated fatty acid
stearidonate (18:4n3)	HMDB06547	0.63	0.0286	0.1075	Lipid	Polyunsaturated fatty acid
trans-4-hydroxyproline	HMDB00725	0.63	0.0004	0.0051	Amino acid	Urea cycle; Arg/Pro metabolism
isovalerylcarnitine	HMDB00688	0.62	0.0478	0.1526	Amino acid	BCAA metabolism
2-hydroxyglutarate	HMDB00606	0.62	0.0054	0.0304	Lipid	Fatty acid, dicarboxylate
1-stearoyl-GPG (18:0)	-	0.62	0.0029	0.0187	Lipid	Lysolipid
1-oleoyl-GPE (18:1)	HMDB11506	0.62	0.0105	0.0506	Lipid	Lysolipid
1-linoleoyl-GPI (18:2)*	-	0.61	0.0011	0.0096	Lipid	Lysolipid
9,10-DiHOME	HMDB04704	0.58	0.0029	0.0187	Lipid	Fatty acid, dihydroxy
gamma-aminobutyrate (GABA)	HMDB00112	0.56	0.0006	0.0075	Amino acid	Glutamate metabolism
2-methylbutyrylcarnitine (C5)	HMDB00378	0.55	0.0027	0.0184	Amino acid	BCAA metabolism
adenosine	HMDB00050	0.54	0.0090	0.0447	Nucleotide	Purine metabolism, adenine containing
dihomo-linolenate (20:3n3 or n6)	HMDB02925	0.52	0.0010	0.0088	Lipid	Polyunsaturated fatty acid
mead acid (20:3n9)	HMDB10378	0.52	0.0157	0.0646	Lipid	Polyunsaturated fatty acid
dihomo-linoleate (20:2n6)	HMDB05060	0.51	<0.0001	0.0006	Lipid	Polyunsaturated fatty acid
isobutyrylcarnitine	HMDB00736	0.50	0.0014	0.0118	Amino acid	BCAA metabolism
1-palmitoyl-GPG (16:0)*	-	0.50	0.0002	0.0032	Lipid	Lysolipid
adrenate (22:4n6)	HMDB02226	0.50	0.0055	0.0306	Lipid	Polyunsaturated fatty acid
5-KETE	HMDB10217	0.49	0.0006	0.0072	Lipid	Eicosanoid
eicosapentaenoate (EPA; 20:5n3)	HMDB01999	0.49	0.0128	0.0577	Lipid	Polyunsaturated fatty acid

docosapentaenoate (n3 DPA; 22:5n3)	HMDB01976	0.46	0.0010	0.0088	Lipid	Polyunsaturated fatty acid
docosahexaenoate (DHA; 22:6n3)	HMDB02183	0.45	0.0010	0.0088	Lipid	Polyunsaturated fatty acid
stearoylcarnitine	HMDB00848	0.44	0.0008	0.0087	Lipid	Acylcarnitine
eicosenoate (20:1)	HMDB02231	0.42	<0.0001	<0.0001	Lipid	Long chain fatty acid
docosadienoate (22:2n6)	HMDB61714	0.40	<0.0001	0.0001	Lipid	Polyunsaturated fatty acid
docosapentaenoate (n6 DPA; 22:5n6)	HMDB01976	0.39	0.0034	0.0208	Lipid	Polyunsaturated fatty acid
erucate (22:1n9)	HMDB02068	0.38	<0.0001	<0.0001	Lipid	Long chain fatty acid
hexanoylcarnitine	HMDB00705	0.33	0.0010	0.0088	Lipid	Acylcarnitine
palmitoylcarnitine	HMDB00222	0.33	0.0027	0.0184	Lipid	Acylcarnitine
linoleoylcarnitine*	HMDB06469	0.29	<0.0001	0.0014	Lipid	Acylcarnitine
myristoleoylcarnitine*	-	0.29	0.0003	0.0040	Lipid	Acylcarnitine
oleoylcarnitine	HMDB05065	0.28	0.0002	0.0032	Lipid	Acylcarnitine
laurylcarnitine	HMDB02250	0.26	0.0001	0.0023	Lipid	Acylcarnitine
myristoylcarnitine	HMDB05066	0.25	0.0003	0.0048	Lipid	Acylcarnitine
palmitoleoylcarnitine*	-	0.22	0.0007	0.0080	Lipid	Acylcarnitine
saccharopine	HMDB00279	0.21	0.0072	0.0378	Amino acid	Lysine metabolism
octanoylcarnitine	HMDB00791	0.20	<0.0001	0.0014	Lipid	Acylcarnitine
4-vinylphenol sulfate	HMDB04072	0.17	<0.0001	0.0003	Xenobiotic	Benzoate metabolism
butyrylcarnitine	HMDB02013	0.11	0.0006	0.0076	Lipid/Amino acid	Acylcarnitine/BCAA metabolism
decanoylcarnitine	HMDB00651	0.10	0.0002	0.0029	Lipid	Acylcarnitine
#campesterol	HMDB02869	0.02	<0.0001	<0.0001	Lipid	Sterol

Metabolites extracted from the hearts of WT and cardiac-specific kd-PFK2 transgenic mice ($Glyco^{Lo}$ mice) were subjected to LC/MS analysis. Raw area counts from each identified metabolite were log-transformed, autoscaled, and then subjected to statistical analyses (t-test). Missing values were imputed using half the minimum value of observed raw area count data, and metabolites with >50% values missing were omitted from the analysis. Asterisks (*) indicate compounds that were not officially confirmed based on a standard, but whose identity matches the expected exact mass using the UHPLC/MS/MS^2 accurate mass platform. Shown are those metabolites with a *p* value threshold of 0.05 and a fold change threshold of 1.25. n = 9 WT mice and n = 10 $Glyco^{Lo}$ mice. #S-methylmethionine was not detected in any of the WT samples, and campesterol was detected only in one WT sample; thus, the relative fold change values are based upon imputed values (i.e., half the minimum value reported for the particular metabolite).

Table S4: Significantly different metabolites in hearts from WT and Glyco^{Hi} mice.

Metabolite	Identifier (KEGG or HMBD)	Relative Fold Change (Glyco^{Hi}/WT)	*p* value	*q* value	Super Pathway	Metabolic Subpathway(s)
cis-4-decenoyl carnitine	-	4.63	0.0060	0.0330	Lipid	Acylcarnitine
linoleoylcarnitine*	HMDB06469	3.38	0.0007	0.0070	Lipid	Acylcarnitine
palmitoleoylcarnitine*	-	3.34	0.0009	0.0080	Lipid	Acylcarnitine
myristoleoylcarnitine*	-	3.27	0.0004	0.0048	Lipid	Acylcarnitine
butyrylcarnitine	HMDB02013	3.26	0.0033	0.0215	Lipid/Amino acid	Acylcarnitine/BCAA metabolism
decanoylcarnitine	HMDB00651	3.07	0.0024	0.0177	Lipid	Acylcarnitine
myristoylcarnitine	HMDB05066	2.63	0.0026	0.0180	Lipid	Acylcarnitine
isovalerylcarnitine	HMDB00688	2.62	0.0018	0.0141	Amino acid	BCAA metabolism
laurylcarnitine	HMDB02250	2.56	0.0016	0.0127	Lipid	Acylcarnitine
1,2-dilinoleoyl-GPE (18:2/18:2)*	-	2.53	<0.0001	<0.0001	Lipid	Phospholipid
palmitoylcarnitine	HMDB00222	2.52	0.0038	0.0226	Lipid	Acylcarnitine
octanoylcarnitine	HMDB00791	2.51	0.0008	0.0075	Lipid	Acylcarnitine
cystathionine	HMDB00099	2.46	<0.0001	<0.0001	Amino Acid	Met, Cys, SAM, Tau metabolism
1-stearoyl-2-linoleoyl-GPE (18:0/18:2)*	-	2.14	<0.0001	<0.0001	Lipid	Phospholipid
1-myristoylglycerol (14:0)	HMDB11561	2.13	0.0247	0.1000	Lipid	Monoacylglycerol
hexanoylcarnitine	HMDB00705	2.08	0.0003	0.0039	Lipid	Acylcarnitine
1-palmitoleoyl-2-linoleoyl-GPC (16:1/18:2)*	-	2.08	<0.0001	<0.0001	Lipid	Phospholipid
oleoylcarnitine	HMDB05065	1.98	0.0099	0.0500	Lipid	Acylcarnitine
stearoylcarnitine	HMDB00848	1.97	0.0030	0.0200	Lipid	Acylcarnitine
1-oleoyl-2-linoleoyl-GPC (18:1/18:2)*	-	1.96	<0.0001	<0.0001	Lipid	Phospholipid
saccharopine	HMDB00279	1.89	0.0037	0.0226	Amino acid	Lysine metabolism
1,2-dilinoleoyl-GPC (18:2/18:2)	-	1.86	<0.0001	<0.0001	Lipid	Phospholipid
isobutyrylcarnitine	HMDB00736	1.85	0.0233	0.0962	Amino acid	BCAA metabolism
2-myristoylglycerol (14:0)	-	1.81	0.0496	0.1649	Lipid	Monoacylglycerol
2-methylbutyrylcarnitine (C5)	HMDB00378	1.77	0.0070	0.0298	Amino acid	BCAA metabolism
1-stearoyl-2-oleoyl-GPC (18:0/18:1)	-	1.76	<0.0001	<0.0001	Lipid	Phospholipid
1-palmitoyl-2-linoleoyl-GPG (16:0/18:2)	-	1.76	<0.0001	0.0008	Lipid	Phospholipid
adenosine 5'-monophosphate (AMP)	HMDB00045	1.76	0.0393	0.1330	Nucleotide	Purine, Adenine containing
glycerophosphoglycerol	C03274	1.74	0.0002	0.0027	Lipid	Glycerolipid
1-oleoyl-2-linoleoyl-GPE (18:1/18:2)*	HMDB05349	1.74	<0.0001	<0.0001	Lipid	Phospholipid
1-palmitoyl-2-arachidonoyl-GPE (16:0/20:4)*	HMDB05323	1.73	<0.0001	<0.0001	Lipid	Phospholipid
beta-hydroxyisovaleroylcarnitine	-	1.72	0.0005	0.0051	Amino acid	BCAA metabolism
1-palmitoyl-2-palmitoleoyl-GPC (16:0/16:1)*	-	1.72	<0.0001	<0.0001	Lipid	Phospholipid
1-palmitoyl-2-linoleoyl-GPE (16:0/18:2)	HMDB05322	1.71	<0.0001	0.0003	Lipid	Phospholipid
1-stearoyl-2-arachidonoyl-GPC (18:0/20:4)	-	1.70	<0.0001	<0.0001	Lipid	Phospholipid
1-arachidonoyl-GPE (20:4n6)*	HMDB11517	1.68	0.0007	0.0071	Lipid	Lysolipid
1-stearoyl-2-linoleoyl-GPC (18:0/18:2)*	-	1.67	<0.0001	0.0001	Lipid	Phospholipid
1-stearoyl-2-arachidonoyl-GPE (18:0/20:4)	-	1.66	<0.0001	<0.0001	Lipid	Phospholipid
1-linoleoyl-2-arachidonoyl-GPC (18:2/20:4n6)*	-	1.64	0.0002	0.0024	Lipid	Phospholipid
erucate (22:1n9)	HMDB02068	1.57	0.0140	0.0661	Lipid	Long chain fatty acid
1-(1-enyl-palmitoyl)-2-arachidonoyl-GPC (P-16:0/20:4)*	-	1.50	0.0004	0.0048	Lipid	Plasmalogen

N6-succinyladenosine	HMDB00912	1.49	0.0488	0.1637	Nucleotide	Purine, Adenine containing
pyridoxal	HMDB01545	1.46	0.0037	0.0226	Cofactor/Vitamin	Vitamin B6 metabolism
benzoate	HMDB01870	1.45	0.0365	0.1330	Xenobiotic	Benzoate metabolism
gamma-aminobutyrate (GABA)	HMDB00112	1.45	0.0067	0.0362	Amino acid	Glutamate metabolism
1-(1-enyl-stearoyl)-2-arachidonoyl-GPE (P-18:0/20:4)*	HMDB05779	1.44	0.0020	0.0146	Lipid	Plasmalogen
oxalate (ethanedioate)	HMDB02329	1.44	0.0012	0.0082	Cofactor/Vitamin	Ascorbate/Aldarate metabolism
stachydrine	HMDB04827	1.44	0.0120	0.0877	Xenobiotic	Food component
1-palmitoyl-2-arachidonoyl-GPC (16:0/20:4)	-	1.44	<0.0001	0.0011	Lipid	Phospholipid
1-palmitoyl-2-linoleoyl-GPC (16:0/18:2)	-	1.42	<0.0001	<0.0001	Lipid	Phospholipid
glycine	HMDB00123	1.41	0.0013	0.0120	Amino acid	Gly, Ser, Thr metabolism
2-oleoylglycerol (18:1)	-	1.41	0.0232	0.0646	Lipid	Monoacylglycerol
1,2-dioleoyl-GPC (18:1/18:1)*	-	1.38	0.0007	0.0071	Lipid	Phospholipid
ornithine	HMDB03374	1.38	0.0260	0.1038	Amino acid	Urea cycle; Arg, Pro metabolism
1-palmitoyl-2-oleoyl-GPC (16:0/18:1)	-	1.37	<0.0001	<0.0001	Lipid	Phospholipid
succinylcarnitine	-	1.37	<0.0001	<0.0001	Energy	TCA cycle
pimelate (heptanedioate)	HMDB00857	1.36	0.0005	0.0053	Lipid	Fatty acid, dicarboxylate
homostachydrine*	HMDB33433	1.36	0.0416	0.1442	Xenobiotic	Food component
N-glycolylneuraminate	HMDB00833	1.35	0.0014	0.0120	Xenobiotic	Food component
cytidine-5'-diphosphoethanolamine	HMDB01564	1.35	0.0052	0.0298	Lipid	Phospholipid metabolism
1-(1-enyl-palmitoyl)-2-linoleoyl-GPC (P-16:0/18:2)*	-	1.33	0.0001	0.0022	Lipid	Plasmalogen
betaine	HMDB00043	1.32	0.0016	0.0127	Amino acid	Gly, Ser, Thr metabolism
2-methylmalonyl carnitine	HMDB13133	1.31	0.0001	0.0023	Lipid	Fatty acid synthesis
4-hydroxy-2-nonenal	HMDB04362	1.31	0.0042	0.0226	Lipid	Fatty acid, oxidized
N6-carboxyethyllysine	-	1.30	0.0038	0.0226	Amino acid	Lysine metabolism
1-(1-enyl-palmitoyl)-2-arachidonoyl-GPE (P-16:0/20:4)*	-	1.29	0.0032	0.0207	Lipid	Plasmalogen
1-stearoyl-2-arachidonoyl-GPI (18:0/20:4)	-	1.29	0.0002	0.0024	Lipid	Phospholipid
sedoheptulose	HMDB03219	1.28	0.0104	0.0519	Carbohydrate	Pentose metabolism
phosphoethanolamine	HMDB00224	1.28	0.0029	0.0198	Lipid	Phospholipid metabolism
asparagine	HMDB00168	1.27	0.0019	0.0141	Amino acid	Ala/Asp metabolism
myo-inositol	HMDB00211	0.79	0.0135	0.0650	Lipid	Inositol metabolism
4-cholesten-3-one	HMDB00921	0.79	0.0022	0.0164	Lipid	Sterol
N1-methyladenosine	HMDB03331	0.78	0.0049	0.0287	Nucleotide	Purine, Adenine containing
1-palmitoyl-GPC (16:0)	HMDB10382	0.77	<0.0001	0.0002	Lipid	Lysolipid
maleamate	C01596	0.77	0.0193	0.0873	Cofactor/Vitamin	Nicotinate/Nicotinamide metabolism
2-piperidinone	-	0.76	0.0127	0.0621	Xenobiotic	Food component
mannose	HMDB00169	0.76	0.0025	0.0180	Carbohydrate	Fructose, mannose, galactose metabolism
N-delta-acetylornithine	-	0.76	0.0094	0.0485	Amino acid	Urea cycle; Arg, Pro metabolism
1-(1-enyl-palmitoyl)-GPC (P-16:0)*	-	0.74	0.0013	0.0114	Lipid	Lysoplasmalogen
stearoyl sphingomyelin (d18:1/18:0)	HMDB01348	0.74	0.0001	0.0023	Lipid	Sphingolipid
sphingomyelin (d18:1/20:0, d16:1/22:0)*	-	0.74	0.0004	0.0045	Lipid	Sphingolipid
citrulline	HMDB00904	0.73	0.0077	0.0375	Amino acid	Urea cycle; Arg, Pro metabolism
1-stearoyl-GPG (18:0)	-	0.72	0.0303	0.1185	Lipid	Lysolipid
hippurate	HMDB00714	0.71	0.0439	0.1484	Xenobiotic	Benzoate metabolism
thiamin (Vitamin B1)	HMDB00235	0.69	<0.0001	0.0007	Cofactor/Vitamin	Thiamine metabolism
fructose	HMDB00660	0.68	0.0035	0.0223	Carbohydrate	Fructose, mannose, galactose metabolism

arabitol/xylitol	-	0.68	0.0204	0.0887	Carbohydrate	Pentose metabolism
dihydroxyacetone phosphate (DHAP)	HMDB01473	0.66	<0.0001	<0.0001	Carbohydrate	Glycolysis
lactate	HMDB00190	0.63	0.0015	0.0120	Carbohydrate	Glycolysis
homocitrulline	HMDB00679	0.62	0.0165	0.0765	Amino acid	Urea cycle; Arg, Pro metabolism
mannitol/sorbitol	HMDB00247	0.59	<0.0001	0.0005	Carbohydrate	Fructose, mannose, galactose metabolism
3-phosphoglycerate	HMDB00807	0.58	0.0200	0.0880	Carbohydrate	Glycolysis
1-palmitoyl-GPG (16:0)*	-	0.58	0.0014	0.0120	Lipid	Lysolipid
1-oleoyl-GPI (18:1)	-	0.48	0.0003	0.0035	Lipid	Lysolipid
carnosine	HMDB00033	0.46	0.0002	0.0024	Peptide	Dipeptide derivative
1-palmitoyl-GPI (16:0)*	HMDB61695	0.46	<0.0001	<0.0001	Lipid	Lysolipid
anserine	HMDB00194	0.45	0.0004	0.0048	Peptide	Dipeptide derivative
phosphoenolpyruvate (PEP)	HMDB00263	0.36	0.0016	0.0127	Carbohydrate	Glycolysis
maltotetraose	HMDB01296	0.27	0.0336	0.1256	Carbohydrate	Glycogen metabolism

Metabolites extracted from the hearts of WT and cardiac-specific pd-PFK2 transgenic mice ($Glyco^{Hi}$ mice) were subjected to LC/MS analysis. Raw area counts from each identified metabolite were log-transformed, autoscaled, and then subjected to t-test analysis. Missing values were imputed using half the minimum value of observed raw area count data, and metabolites with >50% values missing were omitted from the analysis. The asterisk (*) indicates compounds that were not officially confirmed based on a standard, but whose identity matches the expected exact mass using the UHPLC/MS/MS^2 accurate mass platform. Shown are those metabolites with a *p* value threshold of 0.05 and a fold change threshold of 1.25. n = 9 WT mice and n = 10 $Glyco^{Hi}$ mice.

Table S5: Echocardiographic parameters from Glyco^{Lo} and Glyco^{Hi} mice compared with WT controls.

	WT			Glyco^{Lo}			WT			Glyco^{Hi}		
	Mean		SD	Mean		SD	Mean		SD	Mean		SD
HR (bpm)	486	±	22	486	±	26	492	±	52	494	±	38
Endocardial Values												
EDV (µl)	44	±	4	49	±	5*	50	±	4	54	±	7
ESV (µl)	12	±	3	15	±	4	15	±	2	20	±	5**
SV (µl)	32	±	3	34	±	3	35	±	4	34	±	4
EF (%)	72	±	4	70	±	6	70	±	4	63	±	5**
CO (ml/min)	15	±	2	16	±	2	17	±	2	17	±	2
Chamber Diameter												
LVIDd (mm)	3.9	±	0.2	4.0	±	0.3	4.1	±	0.2	4.4	±	0.3*
LVIDs (mm)	2.3	±	0.3	2.3	±	0.3	2.5	±	0.3	2.9	±	0.3**
Wall Thickness												
LVPWd (mm)	0.8	±	0.1	0.9	±	0.1*	1.0	±	0.2	1.0	±	0.1
LVPWs (mm)	1.3	±	0.2	1.4	±	0.2	1.5	±	0.2	1.4	±	0.1
LVAWd (mm)	0.9	±	0.1	0.9	±	0.1	1.1	±	0.2	1.2	±	0.2
LVAWs (mm)	1.3	±	0.2	1.3	±	0.2	1.6	±	0.3	1.6	±	0.2
RWT	0.43	±	0.07	0.47	±	0.10*	0.51	±	0.10	0.45	±	0.07
(n=)	10			10			11			11		

Cardiac structure and function were evaluated in 20-week-old, male, cardiac-specific, kd-PFK2 mice (Glyco^{Lo} mice), pd-PFK2 mice (Glyco^{HI} mice) and WT littermates by echocardiography. Abbreviations: HR, heart rate; EDV, end-diastolic volume; ESV, end-systolic volume; SV, stroke volume; EF, ejection fraction; CO, cardiac output; LVIDd, left ventricular internal diameter in diastole; LVIDs, left ventricular internal diameter in systole; LVPWd, left ventricular posterior wall in diastole; LVPWs, left ventricular posterior wall in systole; LVAWd, left ventricular anterior wall in diastole; LVAWs, left ventricular anterior wall in systole; RWT, relative wall thickness. *$p<0.05$, **$p<0.01$ vs. corresponding WT controls.